Odd−Even Effects and the Influence of Length and Specific Positioning of Alkoxy Side Chains on the Optical Properties of PPE−PPV Polymers

Daniel Ayuk Mbi Egbe,*,† Christoph Ulbricht,† Thomas Orgis,‡ Benjamin Carbonnier,§ Thomas Kietzke,‡ Micha Peip,†,|| Manuela Metzner,|| Martin Gericke,|| Eckhard Birckner,|| Tadeusz Pakula,§ Dieter Neher,‡ and Ulrich-Walter Grummt||

Institut für Organische Chemie und Makromolekulare Chemie der Friedrich-Schiller Universität Jena, Humboldtstr. 10, D-07743 Jena, Germany, Institute of Physics, University of Potsdam, Am Neuen Palais 10, D-14469 Potsdam, Germany, Max-Planck-Institut für Polymerforschung, Ackermannweg 10, D-55128 Mainz, Germany, and Institut für Physikalische Chemie der Friedrich-Schiller-Universität Jena, Lessingstr. 10, D-07743 Jena, Germany

Received July 2, 2005. Revised Manuscript Received September 8, 2005

This contribution reports the combined influences of *odd−even effects* and the *specific* positioning of alkoxy side chains $OR^1 = (OC_{n+10}H_{2(n+10)+1})$ and $OR^2 = (OC_nH_{2n+1})$ (with $n = 6, 7, 8, 9$) on the *phenylene−ethynylene* and *phenylene−vinylene* segments, respectively, on the optical properties of hybrid polymers **P(n+10)/n** of general repeating unit: −Ph−C≡C−**Ph**−C≡C−Ph−CH═CH−**Ph**−CH═CH−. For the polymeric materials, visual color impression varies alternatively between orange red (**P16/6** and **P18/8**) and yellow (**P17/7** and **P19/9**) according to the *odd* and *even* features of the alkoxy side chains, where *odd* or *even* relates to the total number of sp^3-hybridized atoms within the side chains. This side chain related effect is ascribed to both absorptive and emissive behaviors of the polymers on the basis of photophysical investigations in the bulk. Almost identical thin film absorption spectra were obtained for all four materials; however, the photoluminescence of the *odd* polymers, **P16/6** ($\lambda_f = 556$ nm) and **P18/8** ($\lambda_f = 614$ nm), was red-shifted relative to that of their *even* counterparts ($\lambda_f = 535$ nm). Further, the **P18/8** maximum at 614 nm can be readily assigned to excimer emission, as evidenced by the largest Stokes shift (5600 cm^{-1}), largest $fwhm_f$-value (3700 cm^{-1}), and the lowest Φ_f-value of 24%. The strong $\pi-\pi$ interchain interaction in **P18/8**, due to loose alkoxy side chains packing, does not only favor fluorescence quenching but also enable an effective *inter-* as well as *intra*-molecular recombination of the generated positive and negative polarons in electroluminescence, which explains the good EL properties of this polymer irrespective of the solvent used. A voltage-dependent blue shift of the EL spectra of up to 100 nm was observed for **P18/8** devices prepared from aromatic solvents. This red to green EL shift as observed with increasing voltage is assigned to conformational changes of the polymer chains with increasing temperature.

Introduction

Since the initial discovery of electrical conductivity in doped polyacetylene by Shirakawa et al.,[1] enormous progress has been made in the design, synthesis, and detailed studies of properties and applications of π-conjugated polymers.[2] The early problems concerning materials insolubility and infusibility have been thoroughly addressed by introducing flexible alkyl and/or alkoxy side groups in poly(*p*-phenylene-vinylene)s,[3,4] poly(*p*-phenylene)s,[5,6] poly(*p*-phenylene-ethynylene)s,[7,8] and polythiophenes.[9,10] The side chains do not only

* Corresponding author. Tel: (+49)-3641-948267. Fax: (+49)-3641-948202. E-mail: c5ayda@uni-jena.de.
† Institut für Organische Chemie und Makromolekulare Chemie der Friedrich-Schiller Universität Jena.
‡ University of Potsdam.
§ Max-Planck-Institut für Polymerforschung.
|| Institut für Physikalische Chemie der Friedrich-Schiller-Universität Jena.

(1) (a) Shirakawa, H.; Louis, E. J.; MacDiarmid, A. G.; Chiang, C. K.; Heeger, A. J. *J. Chem. Soc., Chem. Commun.* **1977**, 578. (b) Chiang, C. K.; Fischer, C. R.; Park, Y. W.; Heeger, A. J.; Shirakawa, H.; Louis, E. J.; Gau, S. C.; MacDiarmid, A. G. *Phys. Rev. Lett.* **1977**, *39*, 1098. (c) Chiang, C. K.; Druy, M. A.; Gau, S. C.; Heeger, A. J.; Louis, E. J.; MacDiarmid, A. G.; Park, Y. W.; Shirakawa, H. *J. Am. Chem. Soc.* **1978**, *100*, 1013.

(2) (a) Skotheim, T. J., Elsenbaumer, R. L., Reynolds, J. R., Eds. *Handbook of Conducting Polymers*, 2nd ed.; Marcel Dekker: New York, 1998. (b) Hadziioannou, G., van Hutten, P. F., Eds. *Semiconducting Polymers: Chemistry, Physics and Engineering*, 1st ed; Wiley-VCH: Weinheim, Germany, 2000.

(3) (a) Braun, D.; Heeger, A. J. *Appl. Phys. Lett.* **1991**, *58*, 1982. (b) Doi, S.; Kuwabara, M.; Noguchi, T.; Ohnishi, T. *Synth. Met.* **1993**, *57*, 4174. (c) Sarnecki, G. J.; Burn, P. L.; Kraft, A.; Friend, R. H.; Holmes, A. B. *Synth. Met.* **1993**, *55*, 914.

(4) (a) Pfeiffer, S.; Hörhold, H.-H. *Macromol. Chem. Phys.* **1999**, *200*, 1870.

(5) (a) Rehahn, M.; Schlüter, A.-D.; Wegner, G.; Feast, W. J. *Polymer* **1989**, *30*, 1054. (b) Rehahn, M.; Schlüter, A.-D.; Wegner, G.; Feast, W. J. *Polymer* **1989**, *30*, 1060. (c) Vahlenkamp, T.; Wegner, G. *Macromol. Chem. Phys.* **1994**, *195*, 8350. (d) Karakaya, B.; Claussen, W.; Gessler, K.; Saenger, W.; Schlüter, A.-D. *J. Am. Chem. Soc.* **1997**, *119*, 3296.

(6) (a) Kreyenschmidt, M.; Uckert, F.; Müllen, K. *Macromolecules* **1995**, *28*, 4577. (b) Scherf, U.; Müllen, K. *Makromol. Chem., Rapid Commun.* **1991**, *12*, 489.

(7) (a) Giesa, R.; Schulz, R. C. *Makromol. Chem.* **1991**, *191*, 857. (b) Halkyard, C. E.; Rampey, M. E.; Kloppenburg, L.; Studer-Martinez, S. L.; Bunz, U. H. F. *Macromolecules* **1998**, *31*, 8655. (c) Bunz, U. H. F. *Chem. Rev.* **2000**, *100*, 1605.

(8) (a) Weder, C.; Wrighton, M. S. *Macromolecules* **1996**, *29*, 5157. (b) Moroni, M.; Le Moigne, M.; Pham, T. A.; Bigot, J.-Y. *Macromolecules* **1997**, *30*, 1964.

10.1021/cm051437e CCC: $30.25
Published on Web 10/26/2005

Chart 1

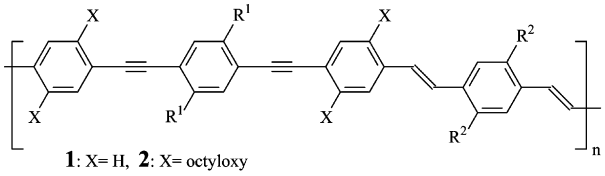

1: X= H, **2**: X= octyloxy

1aa: $R^1 = R^2$ = octadecyloxy. **1ab**: R^1 = octadecyloxy, R^2 = dodecyloxy
1bb: $R^1 = R^2$ = dodecyloxy. **1ac**: R^1= octadecyloxy, R^2 = octyloxy.
1ca: R^1 = octyloxy, R^2 = octadecyloxy. **1ad**: R^1 = octadecyloxy, R^2 = 2-ethylhexyloxy.
1da: R^1 = 2-ethylhexyloxy, R^2= octadecyloxy. **1dd**: $R^1 = R^2$ = 2-ethylhexyloxy.
2aa: $R^1 = R^2$ = octadecyloxy. **2ca**: R^1= octyloxy, R^2 = octadecyloxy.
2cc: $R^1 = R^2$ = octyloxy. **2dd**: $R^1 = R^2$ =2-ethylhexyloxy.

function as solubilizing agents but also play a primordial role in the bulk self-assembling abilities and resulting photophysical and electrochemical properties of the polymers.[11] Attachment of alkoxy side chains to the polymer backbone moreover lowers the optical band gap of most polymers, thereby playing an important role in the color tuning of the polymeric materials. The above-mentioned aspects have been demonstrated in a series of liquid crystalline phenylene-ethynylene-*alt*-phenylene-vinylene hybrid polymers, **1** and **2**, whose general constitutional structure is depicted in Chart 1.[12]

All polymers of type **1** ($\lambda_a = 450$ nm, $\lambda_f = 490$ nm $\Phi_f = 60-70\%$) and those of type **2** ($\lambda_a = 470$ nm, $\lambda_f = 490$ nm, $\Phi_f = 70-80\%$) exhibit similar solution absorption and emission behaviors. The red shift of the absorption and emission spectra of polymers **2** is ascribed to their higher number of alkoxy side chains. The solid state properties (color, absorption, emission, fluorescence quantum yield, photoconductivity, etc.) of these polymers were found to be greatly dependent on the *number*, *position*, *length*, and *geometry* of the grafted alkoxy side chains. Among the first synthesized polymers of type **1**, polymer **1ac**, with side chains R^1 = octadecyloxy and R^2 = octyloxy, is very distinct in its solid-state properties. While all the other polymers are yellow in color, **1ac** is orange red. Its emission spectrum is

Figure 1. Picture of bulk polymeric materials.

Scheme 1

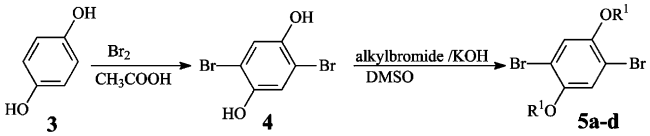

a: R^1= hexadecyl; **b**:R^1= heptadecyl; **c**: R^1= octadecyl, **d**: R^1= nonadecyl.

Scheme 2

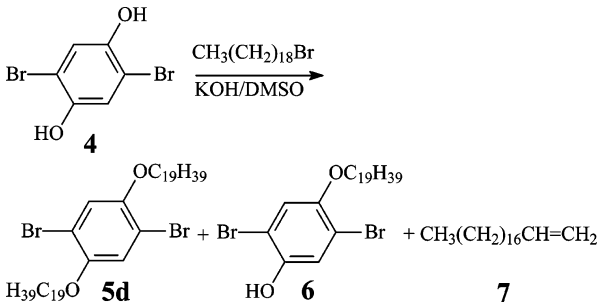

broader and has a maximum centered around $\lambda_f = 602$ nm, which is approximately 90 nm red-shifted compared to those of the other polymers. It is moreover characterized with the highest Stokes shift of 4900 cm^{-1} and lowest Φ_f-value of 19%. To check whether similar photophysical behavior as in **1ac** could be reproduced if other side chains combinations are grafted on the backbone of **1**, two series of polymers of type **1** were synthesized and investigated. In the first series, we kept $R^1 = OC_{18}H_{37}$ constant and varied $R^2 = OC_nH_{2n+1}$ (n = 4, 5, 6, 7, 9, 10, 12, 14, and 16) from butyloxy to hexadecyloxy.[13] In the second series, R^2 was kept equal to octyloxy; dodecyl as well as octadecyloxy groups were attached at R^1.[12,14] Both investigations led to polymers showing similar solid-state characteristics as the polymers of type **1**.[12] The absorption maxima of the yellow compounds are located around $\lambda_a \sim 480$ nm. Their relatively (to **1ac**) narrow emission bands consist either of two peaks, centered at $\lambda_f \sim 510$ nm (highest intensity) and at $\lambda_f \sim 540$ nm, or of one peak located around $\lambda_f \sim 535$ nm and higher and lower energy shoulders. Stokes shift between 2400 and 3400 cm^{-1} and fluorescence quantum yields between 30 and 44% were measured.[12,14]

In the search for an explanation of the outstanding spectral behavior of **1ac**, our focus in this work is directed to the following question: Is it possible to observe similar spectral behavior by keeping the difference of 10 methylene ($-CH_2-$) units between R^1 and R^2 as it is found in **1ac**? How important is the parity (*odd−even effects*) of the alkoxy chains in this case? Odd−even effects of alkyl/alkoxy chains acting as

(9) Sato, M.; Morii, H. *Polym. Commun.* **1991**, *32*, 42. (b) Sato, M.; Morii, H. *Macromolecules* **1991**, *24*, 1196.
(10) (a) McCullough, R. D.; Lowe, R. D.; Jayaraman, M.; Anderson, D. L. *J. Org. Chem.* **1993**, *58*, 904. (b) Chen, T.-A.; Wu, X.; Rieke, R. D. *J. Am. Chem. Soc.* **1995**, *117*, 233.
(11) (a) Shin, C.-K.; Lee, H. *Synth. Met.* **2004**, *140*, 177. (b) Fang, Q.; Yamamoto, T. *Polymer* **2003**, *44*, 2947. (c) Eldo, J.; Ajayaghosh, A. *Chem. Mater.* **2002**, *14*, 410. (d) Wu, Z.; Wu, S.; Liang, Y. *Langmuir* **2001**, *17*, 7267. (e) Bolognesi, A.; Porzi, W.; Provasoli, A.; Botta, C.; Comotti, A.; Sozzani, P.; Simonutti, R. *Macromol. Chem. Phys.* **2001**, *202*, 2586. (f) Chen, Z.-K.; Huang, W.; Wang, L.-H.; Kang, E.-T.; Chen, B. J.; Lee, C. S.; Lee, S. T. *Macromolecules* **2000**, *33*, 9015. (g) Rasmussen, S. C.; Straw, B. D.; Hutchison, J. E. *ACS Symp. Ser.* **1999**, *735*, 347. (h) Egbe, D. A. M.; Nguyen, L. H.; Hoppe, H.; Mühlbacher, D.; Sariciftci, N. S. *Macromol. Rapid. Commun.* **2005**, *26*, 1389.
(12) (a) Egbe, D. A. M.; Tillmann, H.; Birckner, E.; Klemm, E. *Macromol. Chem. Phys.* **2001**, *202*, 2712. (b) Egbe, D. A. M.; Roll, C. P.; Birckner, E.; Grummt, U.-W.; Stockmann, R.; Klemm, E. *Macromolecules* **2002**, *35*, 3825. (c) Egbe, D. A. M.; Bader, C.; Nowotny, J.; Günther, W.; Klemm, E. *Macromolecules* **2003**, *36*, 5459. (d) Egbe, D. A. M.; Bader, C.; Klemm, E.; Ding, L.; Karasz, F. E.; Grummt, U.-W.; Birckner, E. *Macromlecules* **2003**, *36*, 9303. (e). Egbe, D. A. M.; Carbonnier, B.; Ding, L.; Mühlbacher, D.; Birckner, E.; Pakula, T.; Karasz, F. E.; Grummt, U.-W. *Macromolecules* **2004**, *37*, 7451. (f) Ding, L.; Egbe, D. A. M.; Karasz, F. E. *Macromolecules* **2004**, *37*, 6124. (g) Ding, L.; Lu, Z.; Egbe, D. A. M.; Karasz, F. E. *Macromolecules* **2004**, *37*, 10031.
(13) Carbonnier, B.; Pakula, T.; Egbe, D. A. M. *J. Mater. Chem.* **2005**, *15*, 880.
(14) Egbe, D. A. M.; Kietzke, T.; Carbonnier, B.; Mühlbacher, D.; Hörhold, H.-H.; Neher, D.; Pakula, T. *Macromolecules* **2004**, *37*, 8863.

Scheme 3

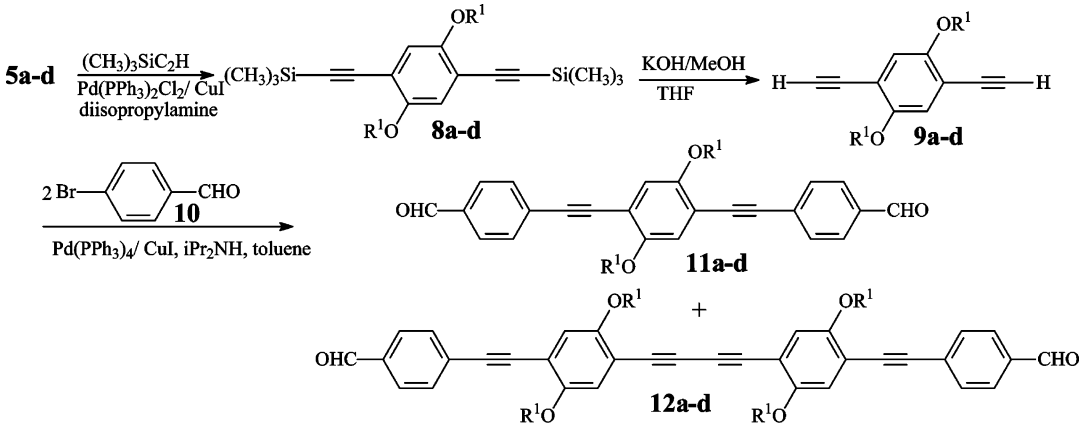

a: R^1 = hexadecyl, **b**: R^1= heptadecyl, **c**: R^1 = octadecyl, **d**: R^1 = nonadecyl.

Scheme 4

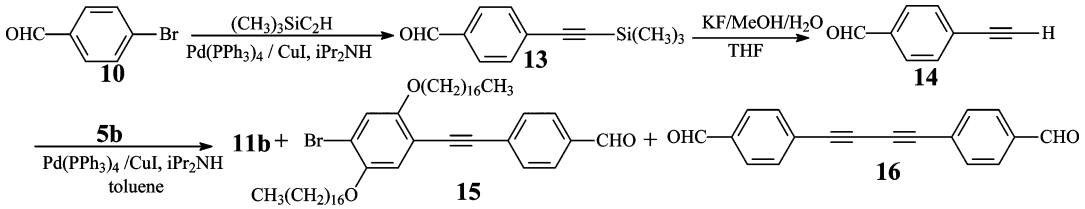

Scheme 5

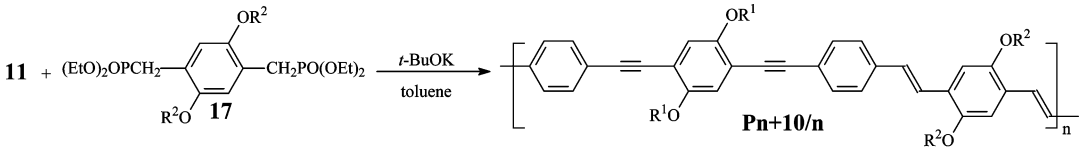

P16/6: R^1 = hexadecyl, R^2= hexyl; **P17/7**: R^1 = heptadecyl, R^2= heptyl; **P18/8**: R^1 = octadecyl, R^2= octyl; **P19/9**: R^1 = nonadecyl, R^2= nonyl

Table 1. Data from GPC (THF, polystyrene standards) and from the DSC. the Heating Rate Was 10 K/min and the Cooling Rate −10 K/min

code	t_R[a] (min)	yield (%)	M_n (g/ mol)	M_W (g/ mol)	M_Z (g/ mol)	M_w/M_n	P	cooling T_{exo}[b] [K]	heating T_{endo}[c] [°C]
P17/7	60	7.3	26 900	111 000	652 100	4.12	24		
P18/8	60	9.8	33 300	64 300	116 600	1.93	28		
P16/6	25	72	16 900	44 600	95 300	2.64	16	356	438.5
P17/7	36	55	28 600	95 400	333 800	3.33	25	357	413
P18/8	37	83	30 600	115 600	517 300	3.77	26	354	383
P19/9	37	89	45 700	171 900	635 300	3.76	37	362	334, 398.5

[a] Reaction time. [b] Exothermic transition temperature. [c] Endothermic transition temperature.

spacers within the main chain or as side groups have been well-documented in other conjugated systems.[15] For instance, *odd*−*even* effect has been recently discussed for side chain dendronized polymers, consisting of regularly segmented alternating rigid-flexible main chain units and side dendritic wedges, showing a periodic variation of bulk characteristics, such as transition temperatures and distances characteristic of the supramolecular structures, as a function of the parity of the main chain spacer.[15g,15h] However, to our knowledge the effect of parity variation of aliphatic segments grafted onto rigid backbones on the structure and related properties of the final "hairy rod" macromolecules has not yet been discussed. The focus so far has been restricted to length, geometry, and grafting density effects.

In this contribution, we report the synthesis and characterization of four new polymers of type **1, P(n+10)/n**, bearing side chains $OR^1 = OC_{n+10}H_{2(n+10)+1}$ and $OR^2 = OC_nH_{2n+1}$ with $n = 6$ for **P16/6**, $n = 7$ for **P17/7**, $n = 8$ for **P18/8**, and $n = 9$ for **P19/9** (Scheme 5). Comparison of their thermal behavior, photophysical, and electroluminescent properties has been carried out and discussed. The parity "*odd*" or "*even*" is related to the total number of sp^3-

(15) (a) Kijima, M.; Kinoshita, I.; Hattori, T.; Shirakawa, H. *Synth. Met.* **1999**, *100*, 61. (b) Grell, M.; Bradley, D. D. C.; Inbasekaran, M.; Woo, E. P. *Adv. Mater.* **1997**, *9*, 798. (c) Mather, P. T.; Jeon, H. G.; Han, C. D.; Chang, S. *Macromolecules* **2002**, *35*, 1326. (d) Mizuno, M.; Hirai, A.; Matsuzawa, H.; Endo, K.; Suhara, M.; Kenmotsu, M.; Han, C. D. *Macromolecules* **2002**, *35*, 2595.(e) Wintgens, D.; Yablon, D. G.; Flynn, G. W. *J. Phys. Chem. B* **2003**, *107*, 173. (e). Auer, F.; Nelles, G.; Sellergren, B. *Chem. Eur. J.* **2004**, *10*, 3232. (f). Pistolis, G.; Andreopoulou, A. K.; Malliaris, A.; Kallitsis, J. K. *J. Phys. Chem. B* **2005**, *109*, 11538. (g) Andreopoulou, A. K.; Carbonnier, B.; Kallitsis, J. K.; Pakula, T. *Macromolecules* **2004**, *37*, 3576. (h) Carbonnier, B.; Andreopoulou, A. K.; Pakula, T.; Kallitsis, J. K. *Macromol. Chem. Phys.* **2005**, *206*, 66.

Table 2. Data from the Absorption and Emission Spectra Obtained in Dilute Chloroform Solution and in Thin Solid Film

code	λ_a[b] [nm]	ϵ_{max}[c] [M^{-1} cm^{-1}]	E_g^{opt} [eV]	λ_f[b] [nm]	$\Delta\nu_{af}$[d] [nm (cm^{-1})]	fwhm$_f$ [nm (cm^{-1})]	Φ_f [%]
15	359	23 300	3.09	468	109 (6500)	93 (4000)	52
11b	396	38 900	2.81	463	67 (3700)	73 (3200)	80
11c	396	40 100	2.81	463	67 (3600)	72 (3200)	80
11d	397	41 500	2.80	464	67 (3600)	73 (3200)	79
P16/6	448	77 600	2.52	*491*, 520	43 (1900)	75 (2800)	65
P17/7	450	101 300	2.53	*490*, 520	41 (1800)	56 (2200)	69
P18/8	450	102 600	2.53	*490*, 520	41 (1800)	58 (2300)	60
P19/9	447	100 000	2.53	*490*, 519	44 (2000)	54 (2100)	71
P16/6[a]	458, *482*		2.37	*556*, 595	74 (2700)	79 (2500)	65
P17/7[a]	458, *483*		2.39	510, *536*, 572	53 (2000)	73 (2400)	54
P18/8[a]	456		2.37	545, *614*	158 (5600)	132 (3700)	24
P19/9[a]	*458*, 478		2.38	514, *535*, 572	78 (3200)	86 (2900)	29

[a] Thin film spin-coated from chlorobenzene. [b] Italic values are the main peaks. [c] Per repeating unit in the case of the polymers. [d] Stokes shift.

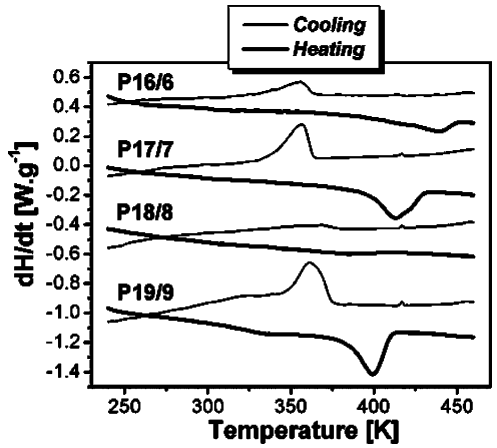

Figure 2. DSC curves of the polymers.

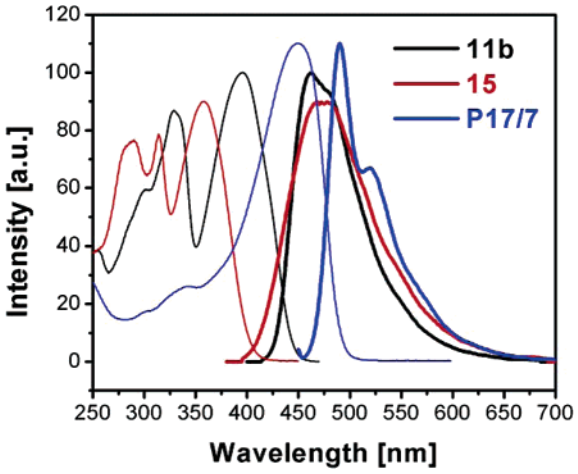

Figure 3. Normalized absorption and emission spectra of dialdehyde **11b**, monoaldehyde **15**, and polymer **P17/7** in dilute chloroform solution.

hybridized side chains atoms (O and C). Consequently, the terms *odd* polymers are used for **P16/6** and **P18/8** and *even* for **P17/7** and **P19/9**.

To elucidate the origin of the different visual color impression (i.e., yellow for **P17/7** and **P19/9** and orange red for **P16/6** and **P18/8**), photophysical properties of the bulk materials, as obtained after polycondensation (Figure 1), were investigated through diffuse reflection and photoluminescence (fluorescence spectra, fluorescence excitation spectra, fluorescence kinetics).

Results and Discussion

Synthesis and Characterization. The synthesis of polymers **P(n+10)/n**, according to the synthetic path described elsewhere by us,[12] requires the preliminary synthesis of luminophoric dialdehydes **11** and bisphosphonate esters **17**. From a retrosynthetic point of view, the dialdehydes can be obtained from two synthetic paths. Whatever synthetic route is chosen, it is necessary to first of all synthesize 2,5-dialkoxy-1,4-dibromobenzene (**5a**−**d**) through the bromination of hydroquinone (**3**)[16] followed by the dialkylation of the obtained 1,4-dibromohydroquinone (**4**)[8a] according to Scheme 1. The "normal" dialkylation reaction is carried out at room temperature due to its exothermic nature. **5a**, **5b**, and **5c** were obtained after a total reaction time of ca. 5 h in yields above 70% after recrystallization. Under this condition only traces of **5d** could be isolated after chromatographic workup; in contrast 44% of the monoalkylated product, 1-hydroxy-2,5-dibromo-4-nonadecyloxybenzene (**6**), was isolated (Scheme 2). Only after elevating the temperature to 50 °C and increasing the reaction time to 48 h could **5d** be obtained in good yield (71%). These "hard" reaction conditions, however, favor the dehydrobromination of nonadecyl bromide, leading to nonadecene-1 (**7**) as shown in Scheme 2. After chromatographic workup, whereby the mixture of **5d** and **7** was separated from traces of **6** and **7** was subsequently separated from **5d** through sublimation.

The first synthetic path to dialdehydes **11a**−**b** is a three-step reaction starting from compounds **5a**−**d** (Scheme 3). Dialdehydes **11a**−**d** were obtained as bright yellow substances in yields between 67 and 82% alongside small amounts (1−6%) of diyne-containing dialdehydes **12a**−**d**, which can also serve as starting materials in additional polycondensation reactions.[17] The second synthetic route to dialdehydes **11**, exemplified here for **11b**, is also a three-step reaction starting from 4-bromobenzaldehyde (**10**) (Scheme 4). The last synthetic step, consisting of the Pd-catalyzed cross-coupling reaction of the dibromo derivative **5b** with 4-ethynylbenzaldehyde (**14**), led to **11b** in a poorer yield of 19% (compared to the first synthetic route). **11b** was obtained

(16) (a) Saraw, E. *Justus Liebigs Ann. Chem.* **1881**, *209*, 108. (b) Bock, H.; Nick, S.; Naether, C.; Bats, J. W. *J. Prakt. Chem.* **1996**, *338*, 363. (c) Pelter, A.; Jenkins, I.; Jones, D. E. *Tetrahedron* **1997**, *53*, 10357.

(17) Egbe, D. A. M.; Birckner, E.; Klemm, E. *J. Polym. Sci., Part A: Polym. Chem.* **2002**, *40*, 2670.

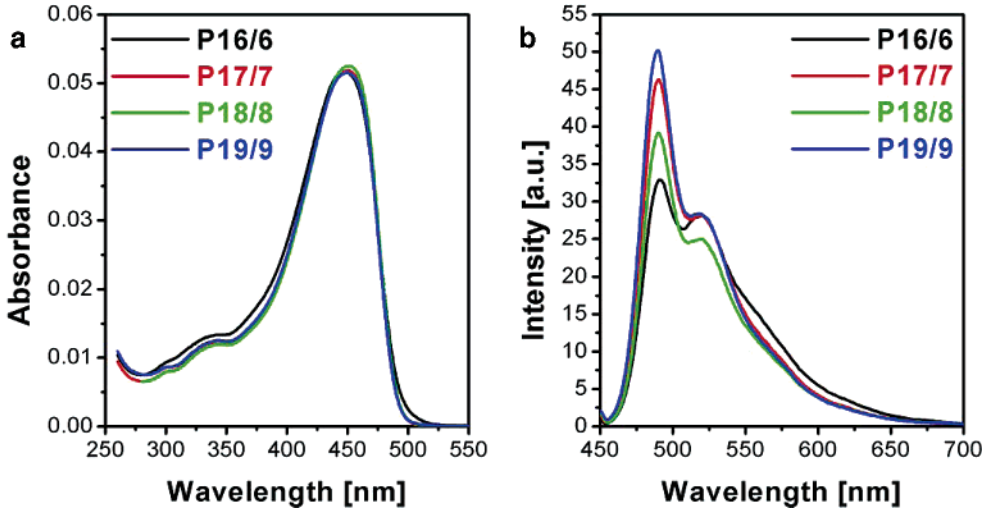

Figure 4. Absorption (a) and corrected emission (b) spectra of the polymers **P(n+10)/n** in dilute chloroform solution.

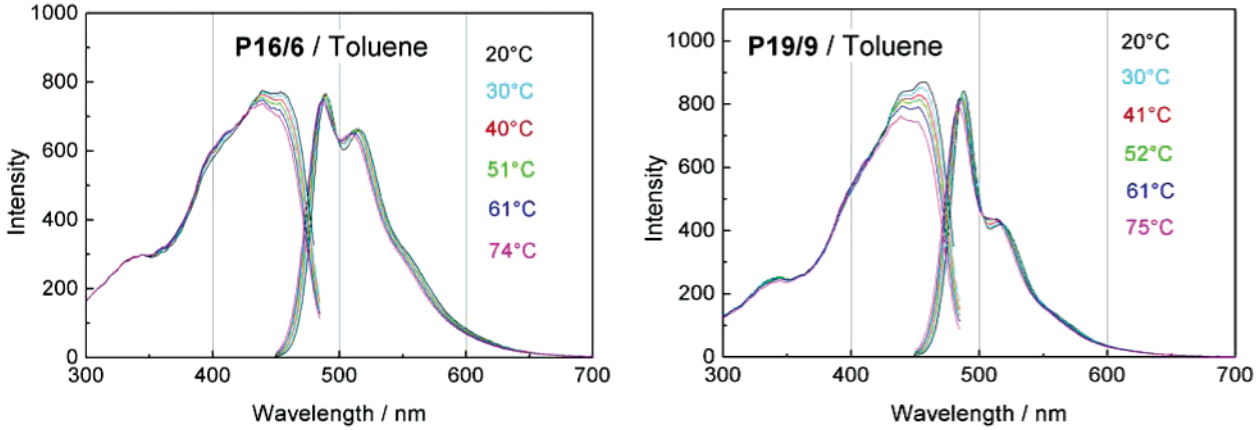

Figure 5. Temperature dependence of fluorescence and fluorescence excitation spectra of **P16/6** and **P19/9** in toluene.

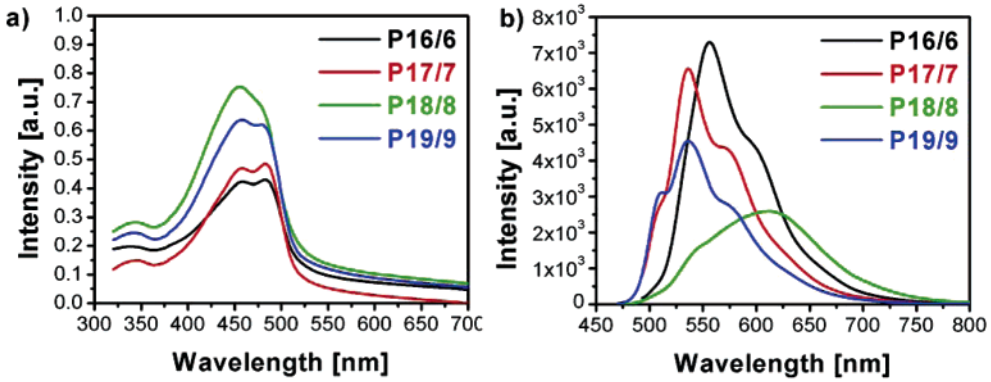

Figure 6. Thin film absorption (a) and emission (b) spectra of the polymers.

alongside the monoethynylated product **15** (13%) and traces of the diyne-containing dialdehyde **16**. The advantage of this reaction route is the comparatively easy chromatographic separation of the three products. The poor yield of **11b** may be assigned to the donor substituents (heptyloxy) on the haloarene **5b**, which do not favor an easy oxidative addition to the electron-rich Pd^0 during the catalytic cycle.[7c] However, an improvement of the yield is expected if bromine is exchanged with iodine.[7c,18] Supporting Information Figures S1 and S2 depict respectively the ^1H NMR and ^{13}C NMR spectra in deuterated chloroform of compounds **15** and **16**.

The polymers **P(n+10)/n** were synthesized according to known procedures,[12] through the Horner-Wadsworth-Emmons olefination reaction of dialdehydes **11** with bisphosphonate esters **17**[13] as shown in Scheme 5. The reaction time was kept below 40 min. Longer reaction time led to lower yields of the soluble portion of the polymers. Data from GPC (polystyrene standards, THF as eluent), reaction times, and yields are given in Table 1. High molecular weight materials were obtained having degree of polymerizations (DP) between 16 and 37 and polydispersity indices between 2 and 4. The *odd* polymers **P16/6** and **P18/8** are orange red in color, whereas the *even* **P17/7** and **P19/ 9** are yellow as shown in

(18) Giesa, R. *J. M. S.-Rev. Macromol. Chem. Phys.* **1996**, *36*, 631.

Table 3. Fluorescence Lifetimes in $CHCl_3$ Solution and Rate Constants of the Deactivation Processes

code	Φ_f[a]	τ[b] [ns]	k_f[c] [ns^{-1}]	k_f (SB)[d] [ns^{-1}]	k_f/k_f (SB)	k_{nr}[e] [ns^{-1}]
P16/6	0.65	0.72	0.90	0.64	1.41	0.49
P17/7	0.69	0.69	1.0	0.83	1.20	0.45
P18/8	0.60	0.68	0.88	0.88	1.0	0.59
P19/9	0.71	0.75	0.95	0.84	1.13	0.39

[a] Fluorescence quantum yield, ±10%. [b] Fluorescence lifetime, ±0.05 ns. [c] Fluorescence rate constant: $k_f = \Phi_f/\tau$. [d] Fluorescence rate constant according to Strickler and Berg:[19] k_f (SB) $= 2.88 \times 10^{-9} \times n^2 \times \int F(\nu)d\nu \times \int \epsilon(\nu)/\nu \, d\nu / \int F(\nu)/\nu^3 \, d\nu$; $\epsilon(\nu)$: absorption coefficient, for the polymers per repeating unit; n, refractive index of the solvent; $F(\nu)$: corrected fluorescence spectrum. [e] Rate constant of radiationless deactivation: $k_{nr} = (1 - \Phi_f)/\tau$.

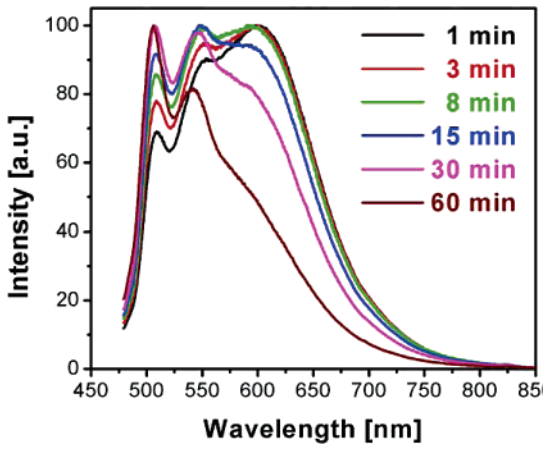

Figure 7. Thin film emission spectra of polymer **1ac** = **P18/8** (M_n = 57 900, M_w = 351 600, polydispersity index: 6.0) as a function of the irradiation time. The sample was excited at the wavelength of the absorption maximum (456 nm).

Figure 1, thereby confirming the fact that *odd−even effects* play an important role in the bulk molecular assembly together with the *difference of 10 methylene* (−CH_2−) units between R^1 and R^2 as well as the s*pecific positioning* of the longer side chains at the phenylene-ethynylene and the shorter side chains at the phenylene-vinylene segments.

Thermal Behavior. Thermogravimetric analysis carried out at a heating rate of 10 K/min under air indicates high thermal stability of the polymeric materials. Thermal decomposition begins between 593 and 623 K, where 5% weight loss was measured. No optically isotropic state was detected using polarizing optical microscopy below the decomposition temperature. The thermal behavior was further examined by means of differential scanning calorimetry (Figure 2). The polymers' endothermic and exothermic peaks are given in Table 1. Both **P17/7** and **P19/9** exhibit sharp endothermic peaks, centered at 413 and 398.5 K, respectively, as well as sharp exothermic transitions, peaked at 357 and 362 K, respectively, suggesting higher ordering and packing mode in these compounds due to the *even effect* of the alkoxy side chains. In contrast, the very broad endothermic peak at 383 K and exothermic peak at 354 K, observed in DSC traces of **P18/8**, can be readily attributed to the *odd effect* of the alkoxy side chains (i.e., loose packing of the side chains). This effect is less pronounced in the case of polymer **P16/6**, which shows some degree of ordering, however of lower intensity than that of **P17/7** and **P19/9**. The differences in the side chains packing mode lead to differences in the conjugated backbone planarization and concomitant $\pi-\pi$ interchain interactions, resulting in differences in color and photophysical as well as electroluminescent properties, as presented and discussed in the following sections.

Photophysical Investigations. The photophysical data of the compounds in dilute chloroform solution and in thin film spin-casted from chlorobenzene are summarized in Table 2, namely, the absorption maximum, λ_a, the absorption coefficient at λ_a, the optical band gap energy, E_g^{opt},[12c] the emission maximum, λ_f, the Stokes shift, $\Delta\nu_{af}$, the full-width-at-half-maximum of the fluorescence, $fwhm_f$, and the fluorescence quantum yield, Φ_f.

Solution. As expected, there is a gradual red shift of the absorption maximum from monoaldehyde **15** (λ_a = 359 nm) over the dialdehyde **11b** (λ_a = 396 nm) to the polymer **P17/7** (λ_a = 449 nm), due to gradual extension of the π-conjugation (Figure 3). The emission band of **15** (λ_f = 468 nm) is slightly broader than that of **11b** (462 nm), suggesting a higher flexibility of the molecule in the S_1 state in **15** than in **11b**. The heavy atom effect (due to the presence of bromine) could be the source of the lower fluorescence quantum yield of **15** (Φ_f = 52%) relative to **11b** (Φ_f = 80%).

Figure 4 presents the absorption and emission spectra in dilute chloroform solution of the polymers. Similar absorption behavior irrespective of the side chains is observed ($\lambda_a \sim$ 450 nm, E_g^{opt} = 2.53 eV). All emission spectra are well-structured and consist of two clear peaks centered at λ_f = 490 and 520 nm. The ratio of the intensity of both peaks are however side chains-dependent. Longer side chains lower the flexibility of the polymeric chains; as a consequence, narrower emission bands are obtained. The intensity of the 520 nm peak is identical in the cases of **P16/6**, **P17/7**, and **P19/9**; a *hypochromic effect* occurs in the case of **P18/8**. Fluorescence quantum yields between 60 and 70% were obtained. The relative high intensity of the 520 nm peak in comparison to the 490 nm one in **P16/6** (having the highest $fwhm_f$-value of 2800 cm^{-1}), might suggest considerable aggregate and/or excimer-like contribution in the emissive process already in the dilute medium. However, temperature-dependent fluorescence measurements, carried out in the range of 30−70 °C in dilute toluene, brought no changes in the emissive behavior as shown in Figure 5, thereby excluding aggregate and/or excimer-like contribution in the radiative process of **P16/6** in dilute media. An additional low-intensity and low-energy discrete shoulder emission band around 560−580 nm was observed in all polymers.

The lack of excimer-like emission in dilute media was also substantiated through kinetic measurements. The fluorescence decay in solution is single exponential with short lifetimes around 0.7 ns with no wavelength dependence. Table 3 summarizes the data from fluorescence kinetics measurements in solution, namely, the fluorescence lifetime, τ, the fluorescence rate constant, k_f, the fluorescence rate constant according to Strickler and Berg,[19] k_f(SB), and the rate constant of radiationless deactivation, k_{nr}. The ratio k_f/k_f (SB) of approximately 1 moreover confirms that the same transi-

(19) Strickler, S. J.; Berg, R. A. *J. Chem. Phys.* **1962**, *37*, 814.

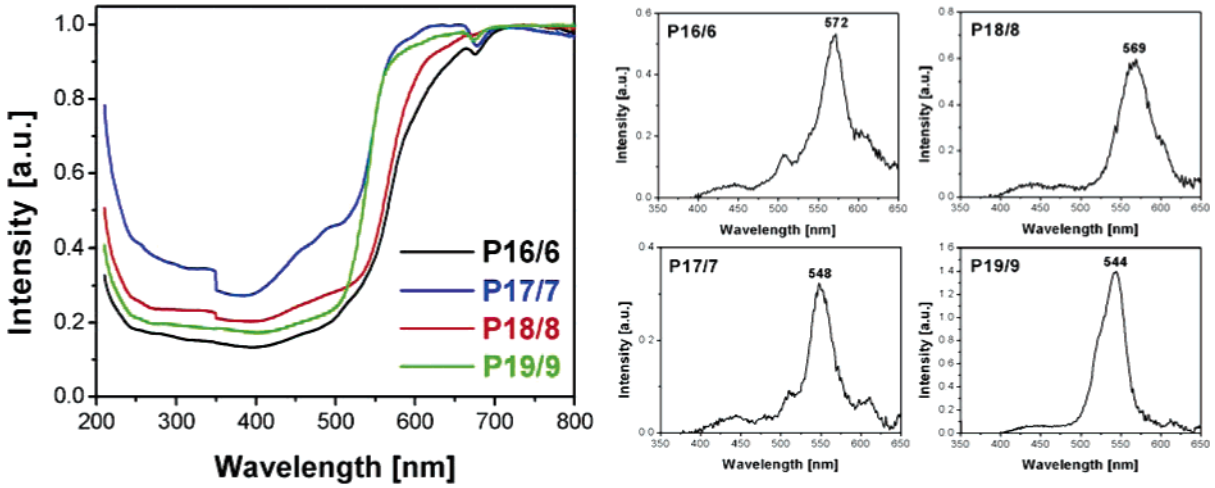

Figure 8. Diffuse reflectance curves (left) and their first derivatives (right) of the polymers.

Table 4. Photophysical Data Obtained from Bulk Compounds as Obtained after Polycondensation

code	$\lambda_{b.dr}$[a] [nm]	λ_{exc}[b] [nm]	$\lambda_{b.exc}$[c] [nm]	λ_f[d] [nm]
P16/6	572	543	570	600
P17/7	548	537	554	579
P18/8	569	548	572	627
P19/9[a]	544	523	547	553, 572

[a] Absorption band edge from diffuse reflectance. [b] Excitation maximum. [c] Band edge of the excitation spectra. [d] Fluorescence maximum.

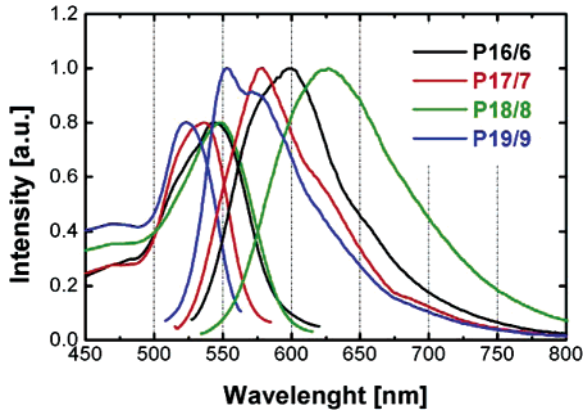

Figure 9. Fluorescence excitation spectra (normalized at 0.8) and fluorescence spectra (normalized at 1.0) of the bulk polymeric materials.

tion is responsible for the absorption and emission.

Thin Film. Figure 6a depicts the thin film absorption spectra of the polymers. Enhanced planarization of the conjugated backbone explains the red shift of the absorption spectra in thin films relative to the solutions. Their main absorption band consists of two maxima, located at around 460 and 480 nm, whereby the 480 nm maximum appears as a discrete shoulder peak in the case of **P18/8**. E_g^{opt} values around 2.40 eV were obtained.

Up to this point (considering the solution absorption and emission and the thin film absorption), only a weak influence of the parity (*odd*−*even* effects) of side chains is observed. These effects appear far more pronounced in the thin film fluorescence of the polymers.

The S_1 state of the *odd* parity polymers, **P16/6** and **P18/8**, is more planarized than that of their *even* parity counterparts, **P17/7** and **P19/9**. This would explain the 20 and 78 nm bathochromic shift of their respective fluorescence spectra [i.e., **P16/6**: $\lambda_f = 556$ nm (sh 0.595 nm); **P18/8**: $\lambda_f = 614$ nm) relative to **P17/7** and **P19/9**, whose emission spectra consist of a maximum at $\lambda_f = 536$ nm and two shoulders around 510 and 570 nm (Figure 6b). The emission spectra of **P17/7** and **P19/9** are indeed more typical of twisted conformation. In contrast, the emission of **P16/6** reminds one of the so-called β phase of poly(dioctylfluorene) which might originate from planar backbone aggregates embedded in a more disordered matrix.[20] The highest fluorescence quantum yield of 65% obtained for **P16/6** would suggest contributions from both "*single-chromophore exciton*" emission and "*aggregates*" emission.[21] "*Aggregates*" emission, as observed in the thin film of alkoxy-substituted CN−PPVs are known to enhance their Φ_f-values.[14,22−24] In contrast, the broad ($fwhm_f = 3700$ cm^{-1}) and structureless emission spectrum of **P18/8** in combination with the lowest Φ_f-value of 24% are clear indications of high contribution from "*excimer*" emission[7c,25,26] in addition to the above-mentioned "*single chromophore* exciton" and "*aggregates*" emissions, resulting from very strong $\pi-\pi$ intermolecular interactions. Fluorescence quenching is a parallel process to *excimer* formation. The **P18/8** emission peak at 614 nm ($\Delta\nu_{af} = 5700$ cm^{-1}) can readily be attributed to "*excimer*" emission, as has been postulated in the past,[12a] and has been confirmed by long time irradiation studies carried out with the first published run of **P18/8** (=**1ac**),[12a] whereby a gradual *hypochromic effect* of the peak at 602 nm and a simultaneous *hyperchromic effect* of the peaks around 510 and 540 nm,

(20) (a) Grell, M.; Bradley, D. D. C.; Long, X.; Chamberlain, T.; Inbasekaran, M.; Woo, E. P.; Soliman, M. *Acta Polym.* **1998**, *49*, 439. (b) Grell, M.; Bradley, D. D. C.; Ungar, G.; Hill, J.; Whitehead, K. S. *Macromolecules* **1999**, *32*, 5810. (c) Cadby, A. J.; Lane, P. A.; Mellor, H.; Martin, S. J.; Grell, M.; Giebeler, C.; Bradley, D. D. C.; Wohlgenannt, M.; An, C.; Vardeny, Z. V. *Phys. Rev. B* **2000**, *62*, 15604.
(21) Chen. S. H.; Su. A.-C.; Huang, Y.-F.; Su. C. H.; Peng, G.-Y.; Chen S. A. *Macromolecules* **2002**, *35*, 4229.
(22) Greenham, N. C.; Samuel, I. D. W.; Hayes, G. R.; Phillips, R. T.; Kessener, Y. A. R. R.; Moratti, S. C.; Holmes, A. B.; Friend, R. H. *Chem. Phys. Lett*. **1995**, *241*, 89.
(23) Samuel, I. D. W.; Rumbles, G.; Collison, C. J.; Moratti, S. C.; Holmes, A. B. *Chem. Phys*. **1998**, *227*, 75.
(24) Tillmann, H.; Hörhold, H.-H. *Synth. Met*. **1999**, *101*, 138.
(25) Rothberg, L. J.; Yan, M.; Papadimitrakopoulos, G., M. E.; Kwock, E. W.; Miller, T. M. *Synth. Methods* **1996**, *80*, 41.
(26) Peng, Z. *Polym. News* **2000**, *25*, 185.

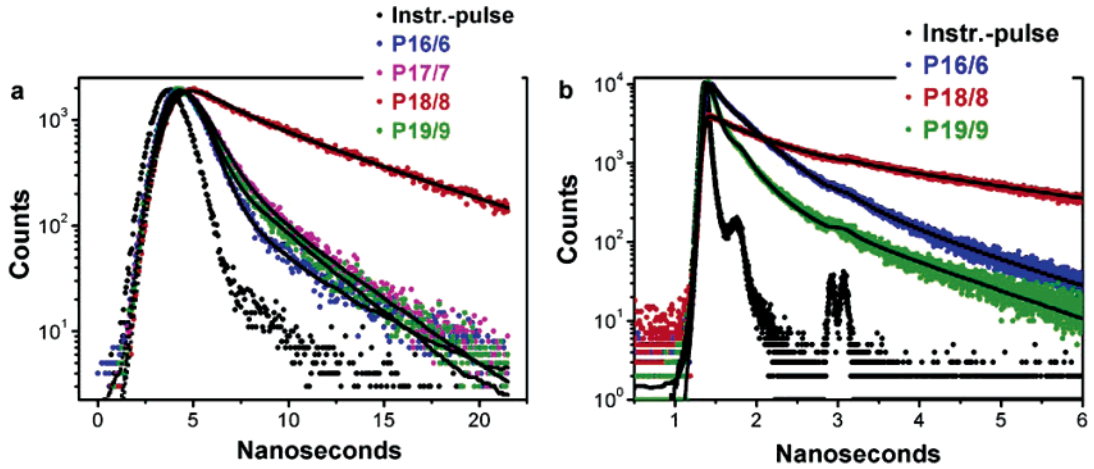

Figure 10. Fluorescence kinetics measurements on solid materials and fitted decay curves with nanosecond excitation at the maximum of the excitation spectrum (left) and with picosecond excitation at 408 nm (right).

attributed to the "*single-chromophore exciton*" emission, were observed (Figure 7). Polymer **P17/7** has the second highest Φ_f-value with 54%, whereas **P19/9** has the second lowest Φ_f-value with 29%, which might be attributed to the differences in the polydispersity indices (PDI). Larger PDI, as in **P19/9**, would open way to more radiationless deactivation channels, thereby lowering the fluorescence quantum yield. This fact is substantiated by our findings on the Φ_f-value of different samples of polymers **1ac**. The higher the polydispersity index, the lower the Φ_f-value; i.e., *sample 1*: $M_n = 14\,000$ g/mol, PDI = 10, $\Phi_f = 12\%$; *sample 2:* $M_n = 12\,000$ g/mol, PDI = 7.6, $\Phi_f = 21\%$; *sample 3*: $M_n = 52\,000$ g/mol, PDI = 7.6, $\Phi_f = 19\%$.

Bulk. Due to the almost identical thin film absorption properties (Figure 6a, Table 2) and the clear differences in the emission properties between the *odd* polymers **P16/6** and **P18/8** and their *even* counterparts **P17/7** and **P19/9**, one might be misled to attribute the differences in color perception (Figure 1) *exclusively* to the emission of these compounds. To make a clear and final statement on this point, we found it necessary to carry out photophysical investigations on the bulk materials, as obtained after polycondensation, as shown in Figure 1 (without externally inducing the orientation and the planarization of the conjugated backbone as is possible during the spin-coating process).

Diffuse reflectance (Figure 8 left) of the bulk materials was obtained with the help of a "Praying Mantis" (PrM) accessory. The maximum of the first derivative of the diffuse reflectance was taken as a measure of the absorption edge (Figure 8 right). An internal integrating sphere was additionally used for comparison. The absorption edges found with the help of this technique coincided with those of the PrM within the reproducibility of about ±2 nm.

Both *odd* polymers **P16/6** and **P18/8** are characterized with ca. 20 nm red-shifted absorption band edges, $\lambda_{b.dr}$, [572 nm (2.16 eV) for **P16/6** and 569 nm (2.17 eV) for **P18/8**] compared with their *even* counterparts, i.e., 548 nm (2.26 eV) for **P17/7** and 544 nm (2.27 eV) for **P19/9** (Table 4).

Figure 9 depicts the fluorescence and the fluorescence excitation spectra of the bulk compounds normalized to 1.0 and 0.8, respectively. The data from the bulk fluorescence studies are given in Table 4. As expected, there is a red shift

Table 5. Results of the Biexponential Curve Fitting[a] of the Fluorescence Kinetics Measurements on Solid Materials, Measured with ns Excitation (fwhm = 1.30 ns), Channel Width: 0.025 ns/Ch, Excited in the Maximum of the Fluorescence Excitation Spectrum

code	$\lambda_{exc}/\lambda_{em}$ [nm]	τ_1 [ns]	ϕ_1 [%]	τ_2 [ns]	ϕ_2 [%]	χ^2
P16/6	540/580	0.67	88	3.57	12	1.01
	540/610	0.71	86	3.53	14	1.01
P17/7	540/580	0.88	73	3.23	27	0.96
	540/610	0.97	73	3.54	27	0.99
P18/8	550/610	2.24	20	7.61	80	1.07
P19/9	525/560	0.58	73	2.80	27	1.11
	525/610	0.75	69	3.33	31	0.98

[a] With $I(t) = B_1e^{-t/\tau 1} + B_2e^{-t/\tau 2}$; $\phi_i = B_i\tau_i/(B_1\tau_1 + B_2\tau_2)$, relative quantum yield of the i-th component.

of the emission maxima going from the thin films to the bulk materials. The excitation maxima of the *odd* polymers **P16/6** and **P18/8** are found at significantly lower energy than those of the *even* ones **P19/9** and **P17/7**. Although not to be expected, the low-energy excitation edges, $\lambda_{b.exc.}$, again measured as the wavelength of the inflection points, agree well with the absorption edges, $\lambda_{b.dr}$, taken from the diffuse reflectance (Table 4). The same ordering is also observed with the emission maxima, although the differences within either group are more pronounced in comparison with the excitation spectra.

We may conclude from these bulk spectral data that the different visual color impression of *odd*- and *even*-numbered polymers is due to both the different absorption and emission behaviors.

Unlike the solution, the fluorescence kinetics in the bulk is complex. The decay curves are generally not single exponential and depend on the selected excitation and emission wavelengths (Figure 10). The powders of the polymers **P16/6**, **P17/7**, and **P19/9** show a similar behavior. The decay curves excited in the long wavelength maximum of the excitation spectra are well-fitted with a biexponential decay law with decay times around 0.8 and 3.2 ns (Table 5). Excitation at shorter wavelength (408 nm) and measurement with picosecond time resolution leads to decay curves which need a triexponential decay law for a good fit (Table 6). The decay times are around 60 ps, 0.33 ns, and 1.3 ns.

Clearly, other values are obtained for **P18/8**, which displays an unstructured and red-shifted fluorescence spec-

Table 6. Results of the Tri-exponential Curve Fitting[a] of the Fluorescence Kinetics Measurements on Solid Materials, Measured with ps Excitation (fwhm = 85 ps), Channel Width: 1.52 ps/Ch, λ_{exc} = 408 nm

code	λ_{em} [nm]	τ_1 [ps]	ϕ_1 [%]	τ_2 [ps]	ϕ_2 [%]	τ_3 [ps]	ϕ_3 [%]	χ^2
P16/6	570	70	16	350	57	1050	27	1.16
	600	108	13	380	60	1160	27	1.15
	650	161	16	440	52	1380	31	1.67
P17/7	580	55	19	350	48	1400	33	1.36
	620	50	14	350	41	1470	45	1.19
P18/8	575	55	12	380	26	2270	62	1.22
	630	73	4	440	20	2550	76	1.07
	660	64	3	445	18	2650	79	1.37
P19/9	550	18	48	240	36	1100	16	1.84
	600	23	23	280	39	1310	25	1.75
	650	29	25	300	40	1540	35	1.76

[a] With $I(t) = B_1e^{-t/\tau}1 + B_2e^{-t/\tau 2} + B_3e^{-t/\tau 3}$; $\phi_i = B_i\tau_i/(B_1\tau_1 + B_2\tau_2 + B_3\tau_3)$, relative quantum yield of the *i*th component.

Table 7. EL Parameters of LED Devices of Configuration ITO/PEDOT:PSS/Pn+10/n/Ca/Al

code	λ_{EL} [nm]	onset voltage [V]	luminance [Cd/m^2]	efficiency [Cd/A]
P16/6[a]	561	3.8	1263 (13.2 V)	0.76
P16/6[b]	558	2.8	1875 (12.2 V)	0.51
P17/7[a]	539	3	1875 (9.7 V)	0.67
P17/7[b]	539	3	2175 (9.7V)	0.99
P18/8[a]	608	2.2	7250 (7.7 V)	1.79
P18/8[b]	643	2.2	4362 (7.7 V)	1.75
P19/9[a]	510, 543	2.4	1850 (9.2 V)	0.48
P19/9[b]	511, 542	3.4	837.5 (11.7 V)	0.41

[a] The active layer was spin-coated from chlorobenzene. [b] The active layer was spin-coated from chloroform.

trum. Also for this sample the kinetics is biexponential or triexponential, respectively, depending on the excitation wavelength, but with a nearly 2-fold increase of the longest decay times (excitation at 550 nm: τ_2 = 7.6 ns, excitation at 408 nm: τ_3= 2.6 ns).

The multiexponential decays could be explained (1) by the heterogeneous nature of the polymeric samples, which consist of chains with different lengths, and (2) by the intermolecular interactions and complexes formations (aggregates or excimers). Excitation at longer wavelength reduces the number of deactivation channels, resulting in the enlargement of the lifetime.

Electroluminescence Investigations. Light-emitting diodes of configuration ITO/PEDOT:PSS/**P(n+10)/n**/Ca/Al were designed and investigated, as described elsewhere by us.[14] The active layers were spin-coated either from aromatic solvents (chlorobenzene, toluene) or from chloroform, to study the influence of solvents in the EL behavior. The EL parameters are given in Table 7. The chlorobenzene electroluminescence spectra (Figure 11) are similar in shape to their corresponding chlorobenzene thin film photoluminescence spectra (Figure 6b), suggesting emission from identical singlet excited states S_1 in both cases.

In the case of **P18/8**, a clear influence of the solvent on the emission spectra could be found. For the aromatic solvents, the emission color depends on the applied bias (Figure 12). At low voltages **P18/8** emits red at around 650 nm. Increasing the applied voltages the emission can be blue-shifted by 100 nm to about 550 nm (green) which is similar to the emission of **P16/6** or **P17/7**. This is so far the largest electroluminescence blue-shift and concomitant change of color among single active layer LED devices at low applied

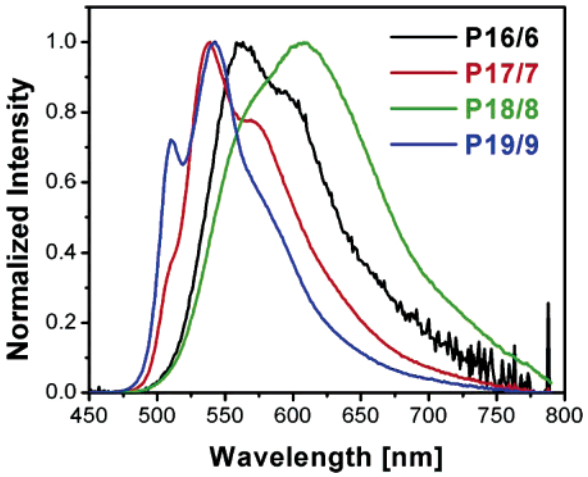

Figure 11. Normalized electroluminescence spectra from devices of configuration ITO/PEDOTL:PSS/polymer/Ca/Al. The active layer was spin-coated from chlorobenzene solution.

voltages.[12e] This process is irreversible; it suggests that the application of higher electric fields and the consequent greater local heating in the polymer film leads to changes in the conformation of the polymer backbone by uplifting the strong $\pi-\pi$ interchain interactions and inducing identical EL behavior in **P18/8** as in **P17/7**.[27] Jenekhe et al.[27] who first reported such irreversible voltage-tunable EL spectra from oxadiazole-containing PPV LED devices, substantiated the above-mentioned explanation by temperature-dependent PL investigations, and this process is termed a "*thermochromic effect*".[12e,27] The same thermochromic effect is at the origin of the changes of the **P18/8** PL spectra, observed during the long time irradiation, as mentioned above. **P18/8** did not show such a blue shift in chloroform. It was also not observed with the other three polymers irrespective of the solvent used while varying the voltage from 3 to 11 V.

Current−voltage and luminance−voltage curves are depicted in Figure 13. **P18/8** exhibited the highest brightness and the highest efficiency compared to the other polymers. A maximum efficiency of 1.8 cd/A was reached for devices using this polymer, nearly independent of the solvent used. This is attributed to the strong $\pi-\pi$ interchain interactions and enhanced planarization, which enable an optimal *intra*molecular as well as *inter*molecular recombination of the generated holes (positive polarons) and the electrons (nega-

(27) Mikroyannidis, J. A.; Spiliopoulos, I. K.; Kasimis, T. S.; Kulkarni, A. P.; Jenekhe, S. A. *Macromolecules* **2003**, *36*, 9295.

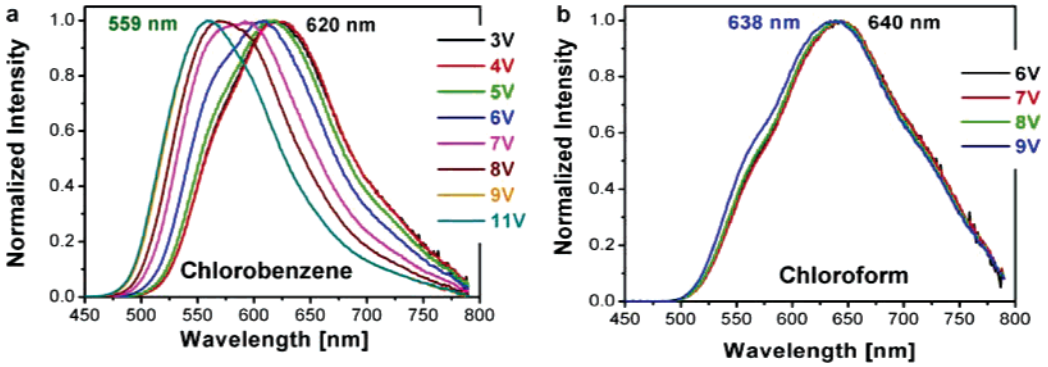

Figure 12. Voltage-dependent EL spectra of polymer **P18/8**. Active layer was spin-coated from either chlorobenzene, toluene, benzene, or chloroform.

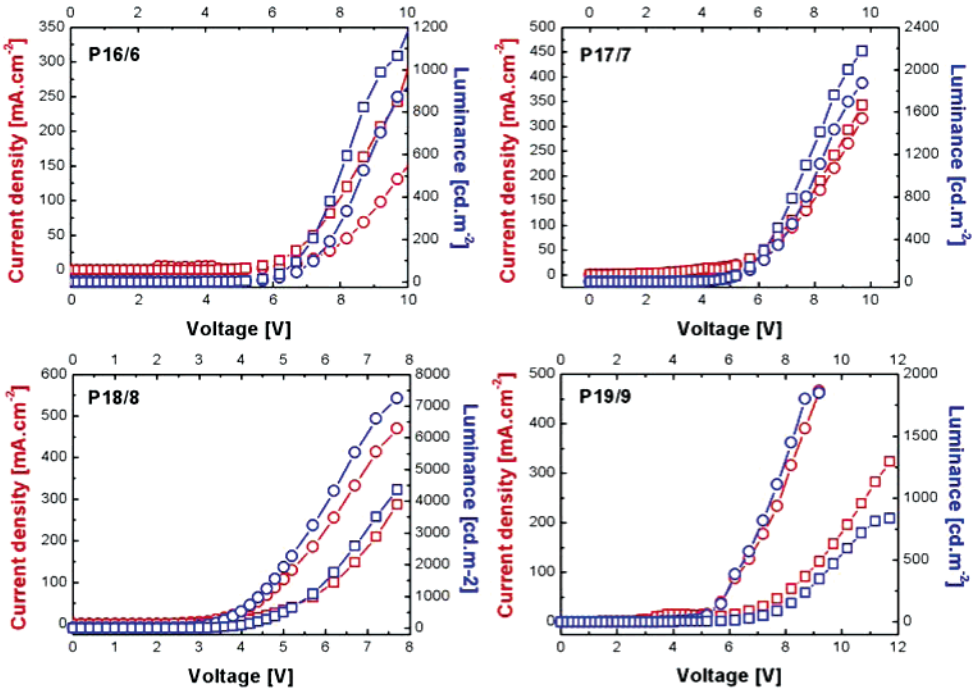

Figure 13. Current density−voltage−luminance characteristics of LED devices of configuration ITO/PEDOT/polymer/Ca/Al. Polymer layer spin-coated from chlorobenzene (○) and from chloroform (□).

tive polarons). The other polymers showed maximum efficiencies of up to 1 cd/A. No significant solvent-dependent efficiency differences were observed for **P16/6**, **P17/7**, and **P19/9**; the efficiency is more dependent on the layer quality.

Conclusions

The synthetic route described here leads to four defect-free alkoxy-substituted PE−PV hybrid polymers, **P(n+10)/n**, combining either *even* or *odd* number of side chains sp^3-hybridized atoms with the *specific positioning* of the longer side chain, $OR^1 = OC_{n+10}H_{2(n+10)+1}$, on the PE-segment, and the shorter chain, $OR^2 = OC_nH_{2n+1}$, on the PV-segment of the macromolecules. Bulk samples of the *odd* polymers **P16/6** and **P18/8** are orange red in color, while their *even* counterparts **P17/7** and **P19/9** are yellow, due to differences in the lateral chains packing and concomitant backbone conformational arrangement as evidenced by DSC measurements. All 4 polymers exhibit identical absorptive behavior in dilute solution; however, the relative intensity of the 490 nm peak and the 520 nm peak of the corresponding emission spectra are polymer-specific. All 4 compounds show almost similar absorptive behavior as thin films. The thin film emission maxima of the *odd* parity polymers **P16/6** and **P18/8** are red-shifted relative to their *even* parity counterparts. **P16/6** exhibits the highest Φ_f-value, suggesting the contribution of *single chromophore excitons* as well as *aggregates* in the radiative process. **P18/8**, on the contrary, exhibits the lowest Φ_f-value resulting from considerable excimer emission. The difference in color perception is due to both a shift of the absorption and the emission of the polymers.

The polymers investigated are useful for the design of light-emitting diode devices of the configuration ITO/PEDOT/polymer/Ca/Al. **P18/8** gives the best EL-parameters despite its lowest Φ_f-value, suggesting an effective *intra*- as well as *inter*-molecular recombination of the generated positive and negative polarons, as a result of the strong π-π interchain interactions.

Films of **P18/8** cast from aromatic solvents (chlorobenzene and toluene) exhibit a ca. 100 nm blue shift of the EL spectra from red (∼650 nm) to green (∼550 nm) (corresponding to

the EL spectra of either **P16/6** or **P17/7**) when the applied bias increased from 3−6 V to 9−11 V. This results from conformational changes of the polymer backbone with increase in local temperature. This same thermochromic effect occurs when long time irradiation of **P18/8** thin film is carried out. The irreversibility of this process proves that the main emission peak of **P18/8** in thin film as well as in bulk (around 600−650 nm) is of *inter*molecular nature rather than of *intra*molecular one.

Supporting Information Available: The experimental description, the synthesis and characterization of the materials, and the ^{13}C NMR spectra of compounds **15** and **16**. This material is available free of charge via the Internet at http://pubs.acs.org.

CM051437E